Global Change Biology

Global Change Biology (2011) **17**, 3312–3326, doi: 10.1111/j.1365-2486.2011.02477.x

Tree mortality in the eastern and central United States: patterns and drivers

MICHAEL C. DIETZE* and PAUL R. MOORCROFT†

*Department of Plant Biology, University of Illinois, Urbana-Champaign, Urbana, IL, USA, †Department of Organismic and Evolutionary Biology, Harvard University, Cambridge, MA, USA

Abstract

Substantial uncertainty surrounds how forest ecosystems will respond to the simultaneous impacts of multiple global change drivers. Long-term forest dynamics are sensitive to changes in tree mortality rates; however, we lack an understanding of the relative importance of the factors that affect tree mortality across different spatial and temporal scales. We used the US Forest Service Forest Inventory and Analysis database to evaluate the drivers of tree mortality for eastern temperate forest at the individual-level across spatial scales from tree to landscape to region. We investigated 13 covariates in four categories: climate, air pollutants, topography, and stand characteristics. Overall, we found that tree mortality was most sensitive to stand characteristics and air pollutants. Different functional groups also varied considerably in their sensitivity to environmental drivers. This research highlights the importance of considering the interactions among multiple global change agents in shaping forest ecosystems.

Keywords: acid rain, Bayesian logistic regression, climate, forest inventory and analysis, nitrogen deposition, ozone, plant functional type, topographic moisture

Received 14 March 2011 and accepted 6 May 2011

Introduction

Tree mortality rates are one of the key factors controlling the long-term dynamics of forest ecosystems. As rates of mortality in forests are generally low, the consequences of changes in mortality rate are not often readily apparent and it can be difficult to identify changes in mortality rate due to the small sample size of deaths within individual studies. Still, life cycle analyses have repeatedly shown that the persistence of long-lived species in general, and trees in particular, is highly sensitive to changes in adult mortality rate (Franco & Silvertown, 1996; Caswell, 2001). Small changes in mortality rate can have large impacts on the lifespan of trees, biodiversity and the cycling of carbon and nutrients. Indeed, tree mortality is a primary driver of changes in forest communities and can cause marked changes in composition and structure. The occurrence of large-scale die-off events, such as the loss of >1.2 million ha of pinyon pine forest in the southwestern United States following the 2002–2003 drought (Breshears *et al.*, 2005), demonstrates the dramatic effects of tree mortality on forest dynamics and the potential for mortality to drive the large-scale reorganization of ecosystems. In a global review of drought and heat stress mortality, Allen *et al.* (2010) suggest that both episodic die-off events and background mortality rates may be increasing globally, but that uncertainties in the patterns and drivers of mortality hinder our ability to anticipate the 'tipping points' for large-scale die-off. However, outside of discrete disturbance events (e.g. fire, windthrow), our current understanding of the patterns and drivers of tree mortality is largely limited to fine-scale processes (e.g. competition, self-thinning), and thus is inadequate to understand how mortality rates will respond to changes in drivers at larger spatial scales.

The simultaneous impacts of climate change, elevated CO_2, acid rain, nitrogen deposition, ozone pollution, land-use change and invasive species create substantial uncertainty about what future ecosystems will look like and how they will function. The fate of forests is of particular interest because they cover almost 4 billion ha world wide and provide important ecosystem services (FAO, 2007). These include the uptake and storage of atmospheric CO_2, habitat for two-thirds of the world's species and the regulation of moisture and nutrient runoff. Forests also have high economic value for wood products, fiber, fuel, and recreation.

Understanding the impacts of global change on forests requires understanding the diverse array of agents that are responsible for spatial and temporal variation in tree mortality rates. At regional scales, vegetation is controlled by climate (Köppen, 1931; Holdridge, 1967), while at the landscape scale, it is affected by heterogeneity in the physical properties of the land surface, in particular the effects of topography and soils on local

Correspondence: Michael C. Dietze, tel. +1217 265 8020, fax +1217 244 2057, e-mail: mdietze@illinois.edu

microclimates, soil biogeochemistry, and hydrology (Whittaker, 1956). At finer spatial scales, vegetation is responding to biotic processes such as competition, herbivory, mutualism, and disease. Likewise, anthropogenic forcings occur at a multitude of spatial scales, ranging from fine-scale patterns of land-use and harvesting, to meso-scale patterns of atmospheric pollutants, to global-scale changes in climate. Understanding regional-scale dynamics of vegetation in general and the long-term (decadal-century) dynamics of forest ecosystems in particular, requires that we understand the relative importance of drivers that operate at very different spatial scales. A number of studies have explored regional-scale patterns in important ecosystem processes, such as variation in NEE (Baldocchi, 2008), NPP (Running *et al*., 2004), leaf traits (Wright *et al*., 2004), and litter decomposition (Gholz *et al*., 2000). However, relatively little is known about regional-scale variability in tree mortality rates, the factors underlie these patterns, and the relative importance of drivers at different spatial scales. A few important exceptions include the RAINFOR plot network in Amazonia (Phillips *et al*., 2004) and a recent study of old growth forest in the northwest United States (van Mantgem *et al*., 2009) both of which suggest increases in background mortality rate due to climate change. The RAINFOR plots also suggest the existence of large-scale gradients in mortality rates driven by soil fertility, with the counterintuitive result that mortality is highest on the most fertile sites (Phillips *et al*., 2004).

At large spatial scales, estimates of tree mortality from national forest inventories have traditionally focused on calculating county-level loss rates for biomass or timber volume rather than per capita mortality risk (e.g. Smith *et al*., 2002). Brown & Schroeder (1999) found no clear spatial pattern of woody biomass mortality for the eastern United States, except for the impact of Hurricane Hugo (1989) on South Carolina. By contrast, analyses of individual-tree mortality rates have generally occurred at small-scales and have focused on individual and stand-level factors such as tree size, growth rate, and neighborhood crowding. With the exception of disturbance events, stand-level studies are unable to assess the impacts of most global change drivers because they can only observe a small range of conditions. Due to the high survivorship among trees the number of observed mortality events in small-scale studies is low, leading to substantial uncertainty in predictions. Larger-scale estimates of individual-level risk have been produced at the scale of individual states (Woodall *et al*., 2005a,b) and small countries (e.g. Monserud & Sterba, 1999; Eid & Tuhus, 2001; Fridman & Stahl, 2001); however, these have likewise primarily focused on tree and stand-level factors.

Questions regarding the potential for rapid 'tipping point' changes in forest ecosystem composition and structure are, at their heart, questions about tree mortality. To anticipate this type of change within regional- and global-scale vegetation models requires improved understanding of the patterns and processes affecting mortality at large spatial scales. The current generation of ecosystem models, despite a large investment in understanding photosynthesis and growth, generally take relatively simple approaches to mortality, such as assuming a constant fraction of biomass loss (e.g. King *et al*., 1997; Thornton *et al*., 2002), or a phenomenological correlation with growth rate (e.g. Smith *et al*., 2001) or carbon balance (e.g. Moorcroft *et al*., 2001). Likewise, in a review of the treatment of mortality in detailed gap models, Keane *et al*. (2001) found mortality was usually represented by simple growth-dependent functions (e.g. Pacala *et al*., 1996; Wyckoff & Clark, 2000) which they similarly found inadequate. These relationships do not scale well, varying among sites or with soil resources, even within a species (Kobe, 1996).

Here we present an analysis of individual-level tree mortality rates across the eastern and central United State based on long-term forest inventory data from the USFS Forest Inventory and Analysis (FIA). This study explicitly addresses the impact of a number of important drivers operating across a hierarchy of four spatial scales: regional-scale climate, meso-scale atmospheric pollutants, landscape-scale variation in topography and hydrology, and stand-scale biotic dynamics. Below, we begin by laying out a series of *a priori* hypotheses regarding the importance of specific drivers at different scales. We then report whether these drivers conformed to our *a priori* hypotheses and evaluate the simultaneous effects of different variables at different scales. Finally, the sensitivity of mortality rate to each driver is calculated and covariates are ranked by their relative impact on mortality and potential global change implications. While many of these covariates have been studied individually, the quantitative understanding of their magnitudes, combined effects, sensitivities, and regional extent afforded by this study is novel and critical for both improved prediction of future forest dynamics and assessing future research priorities.

Covariate hypotheses

The aim of this section is to present the hypothesized responses for each of the 13 covariates spanning four spatial scales: regional-scale climate, meso-scale atmospheric pollutants, landscape-scale variation in topography and hydrology, and stand-scale biotic dynamics.

At the regional climate scale, we examine the effects of mean annual precipitation, mean summer maximum

temperature, and mean winter minimum temperature. For precipitation, we hypothesize that: (i) mortality will decrease with increasing precipitation because plants will experience less moisture stress and less frequent droughts; (ii) angiosperms will be more sensitive to moisture than gymnosperms because the later tend to have more drought adaptations and a lower likelihood of cavitation due to their smaller vessel sizes (Maherali *et al*., 2004; Sperry *et al*., 2006); and (iii) late successional species will be adapted to shade conditions that are moister and thus have higher sensitivity to precipitation. For winter temperatures, we hypothesize that: (i) mortality will increase as temperatures get colder due to an increase in frost damage; and (ii) midsuccessional hardwoods, which are dominated by ring-porous genera such as oaks, will be most sensitive to cold winters due to their greater propensity for freeze embolism while ring-diffuse angiosperms will be intermediate and conifers will be least sensitive (Sperry & Sullivan, 1992). Alternately, tree mortality may increase as winter temperatures get warmer if pests escape winter mortality or the need for winter dormancy (Kliejunas *et al*., 2009). In this case, we hypothesize that gymnosperms will be more sensitive to warm winters because of their higher load of endemic pests (e.g. Southern pine beetle *Dendroctonus frontalis*, spruce budworm *Choristoneura fumiferana*). For summer temperatures, we hypothesize that mortality will decrease with increased temperature because of increasing growing season length and NPP (Baldocchi, 2008). However, increased temperature also incurs the cost of higher respiration costs, higher heat stress, and higher risk of cavitation (McDowell *et al*., 2008; Allen *et al*., 2010), and thus could also result in increased mortality with increasing temperature.

The second group of covariates investigated were atmospheric pollutants, specifically nitrogen (N) deposition, acid deposition, and ozone. For N deposition, we hypothesize that mortality rates will decrease with increasing deposition due to fertilization, but at high levels of N deposition, mortality will increase due to N saturation and soil acidification (Magill *et al*., 2004). Furthermore, we expect that early successional species will be most sensitive to N deposition due to their higher nutrient demand (Shinano *et al*., 2001; Wright *et al*., 2004). For both acid deposition and ozone, we predict a consistent increase in mortality for all species. The impacts of acid deposition come from two primary mechanisms. The first is the direct impact on foliage, which is particularly strong among high-elevation species such as red spruce (*Picea rubens*) that are subject to acid fogs and freezes, while the second impact is a general mobilization of soil base cations (in particular Ca^{2+}, Mg^{2+}, and K^{+}) that results in a transient fertilization effect followed by a long-term decline due to nutrient leaching and plant deficiencies (Tomlinson, 2003). The latter effect appears to be having the greatest immediate impact on sugar maple (Acer saccharum), whose populations are predicted to be in decline (Kobe *et al*., 2002). The impacts of ozone occur from damage to the photosynthetic apparatus as determined by the cumulative absorption through leaf stomata, and thus differences among taxa and environments should relate to differences in stomatal conductance (Reich, 1987). Meta-analysis shows that photosynthetic rates of angiosperms are more affected by ozone than conifers and that there are clear differences among genera (Wittig *et al*., 2007), however, these differences do not appear to map neatly onto successional status.

The third category considered was topography, including elevation, slope, and topographic variation in solar radiation and soil moisture. While the direct effects of elevation are negligible, there are numerous indirect effects correlated with elevation (Körner, 2007) such as fine-scale microclimate and pollutant effects not captured by the large-scale data on climate and pollution concentrations. As a result of the decrease in temperature and increase in atmospheric pollutants and wind stress, we predict that mortality will increase with elevation despite increases in precipitation. These predictions are specific to the comparatively moist and rolling eastern United States, and would not be expected to hold in other regions, for example for much of the western United States where the effects of elevation may be driven more by changes in water stress and fire risk. We also predict that mortality rates will increase with increasing slope due to decreases in the retention of soils and moisture and the greater risk of uprooting. For solar radiation, we hypothesize that mortality may be lower on exposed southern slopes, and highest on shadowed northern slopes due to light limitation effects on NPP; alternately this pattern may be reversed if radiation-driven increases in evaporative loss rates resulted in increased drought stress. Finally, since drought-induced die-offs generally affect dry microsites first (Allen *et al*., 2010), we hypothesize that areas with higher soil moisture experience lower mortality rates due to an alleviation of moisture stress. However, droughts may instead have a larger impact on moist microsites if shallower rooting depths leave trees on these sites more vulnerable than deep rooted trees on dry sites (Elliott & Swank, 1994).

The fourth set of drivers considered were biotic interactions, in particular the impacts of stand basal area, stand age, and focal-tree diameter at breast height (DBH). Numerous studies have suggested an increase in mortality with basal area due to an increase in competition (Monserud & Sterba, 1999; Woodall *et al*., 2005a,b; Shifley *et al*., 2006) and we hypothesize that

these effects will be strongest in early successional species. We also hypothesize that the effects of stand age will vary across successional stage, with early successional species showing declines in survival with age while late successional species are expected to have a low sensitivity to age. For tree diameter, we hypothesized that tree mortality would follow a reverse J-shaped curve, with high mortality among juveniles, low mortality for canopy trees, and slowly increasing mortality for the largest trees during senescence (Vieilledent *et al.*, 2009, 2010).

Methods

Study region

The study region considered consists of the eastern and central portions of the continental United States, bounded to the west by 98°W longitude (Fig. 1). This region encompasses the eastern temperate deciduous and conifer forests in the United States, as well as subboreal forest along the northern edge, subtropical vegetation in southern Florida, and shrubland along the southwestern edge.

Forest inventory data

Both the mortality data and a number of covariates were extracted from the US Forest Service's FIA database (http://www.fia.fs.fed.us/, version 2.1). Data were selected from the period 1971–2005, with the sampling design varying slightly among regions during the early phase of data collection before national standardization in 1999. Inventory plot locations are selected based on remote sensing data at a density of approximately one plot per 2400 ha and consist of four circular 7.3 m radius subplots per plot. Within each subplot, all trees over 12.7 cm DBH (measured at 1.37 m) are identified and measured, while saplings measuring 2.54–12.6 cm DBH are only measured in a 2.07 m radius microplot within each subplot. Plot re-measurement frequency has varied historically, averaging approximately once per decade with most plots being remeasured every 5–15 years. In the new standardized design, 20% of the plots are remeasured every year, yielding a median 5-year return interval. Here, we make use of the following tree and plot-level variables: tree survival, species, DBH, plot basal area ($m^2\ ha^{-1}$), age (years), re-measurement period (years), elevation (meters), slope (%), aspect (degrees), latitude and longitude (degrees). A topographic radiation index was calculated from slope and aspect as cos(aspect)*slope/100 and is zero for a flat surface, negative for a southern exposure and positive for a northern exposure. Data were extracted at the individual level and excluded trees that were not remeasured in consecutive censuses, were removed by harvest, or had missing data. The total sample size consisted of ca. 3.4 million tree measurements and over 750 000 plot measurements.

The values of all stand-scale structural and topographic covariates except Topographic Convergence Index come directly from the FIA plot measurements, while the values of all other covariates (described below) were obtained by aligning the spatial coordinates of the FIA plots with corresponding data layers. The latitudes and longitudes of all FIA plots are only available with limited accuracy, corresponding to ca. 800 m error in each plot's latitude and longitude. Climate and atmospheric pollutant variables are highly spatially autocorrelated at the kilometer-scale and thus the spatial accuracy

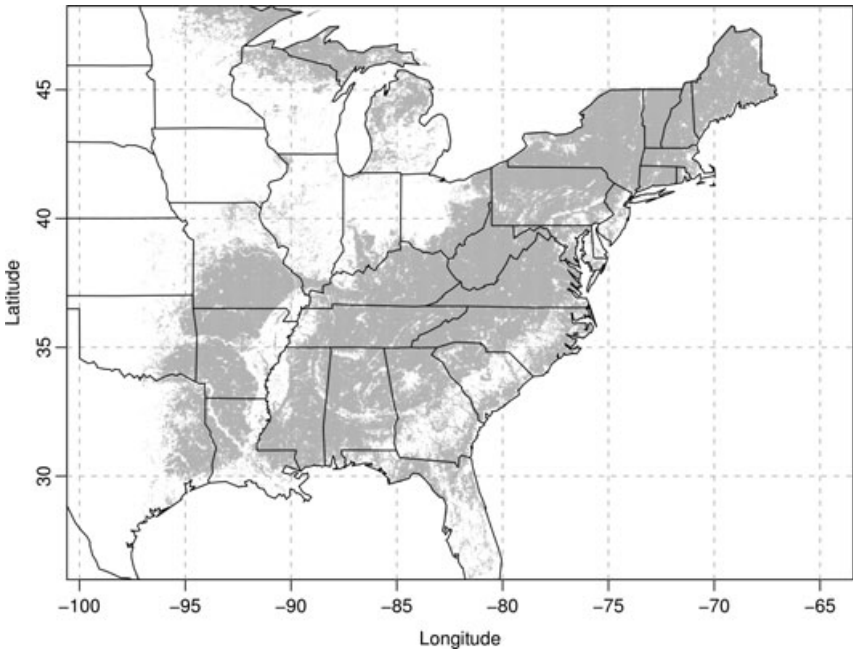

Fig. 1 Study region focuses on eastern temperate forest and consists of the continental United States east of −98°W longitude. Shading indicates the distribution of forest within the region based on the National Land Cover Database 2001 (http://www.mrlc.gov/).

of the climate and air pollution datasets is similar to that of the FIA plot locations. For these covariates, it was therefore possible to use publicly available uncorrected FIA coordinates to extract plot-level values for the climate and air pollution datasets. The alignment and extraction were perfomed using the GRASS GIS software package (GRASS Development Team, 2007). For the landscape-scale topographic covariates that vary on a much finer spatial scales, extraction was performed using by the FIA's Spatial Data Services office (http://www.fs.fed.us/ne/fia/spatial/index_ss.html) using the exact location data for each FIA plot.

Climate

Climate data for the region were extracted from the 800 m resolution PRISM database (http://www.prism.oregonstate.edu/index.phtml). PRISM is a sophisticated interpolation of meteorological station data that accounts for location, elevation, coastal proximity, topographic facet orientation, vertical atmospheric layer, topographic position, and orographic effectiveness of the terrain (Daly *et al.*, 2008). Using data from 1971 to 2000, we extracted the annual average precipitation (ppt), the average monthly minimum temperature across December, January, and February (T_{min}DJF), and the average monthly maximum temperature across June, July, and August (T_{max}JJA). Precipitation rates ranged from ca. 500 to 2500 mm yr^{-1} with a weak northwest to southeast gradient, while DJF minimum temperature varies from ca. −20 to 15 °C and JJA maximum temperature varies from roughly 20 to 35 °C, with both temperature variables showing a marked north–south gradient (Fig. 2a–c). The three climate proxies are significantly correlated, with correlation coefficients of 0.82 between of T_{min}DJF and T_{max}JJA, 0.83 between T_{min}DJF and ppt, and 0.51 between T_{max}JJA and ppt.

Atmospheric pollutants

Data on the atmospheric pollutant covariates came from two sources. The National Atmospheric Deposition Program (http://nadp.sws.uiuc.edu) provides annual maps of the wet deposition (kg ha^{-1}) of ammonium (NH_4^+), nitrate (NO_3^-),

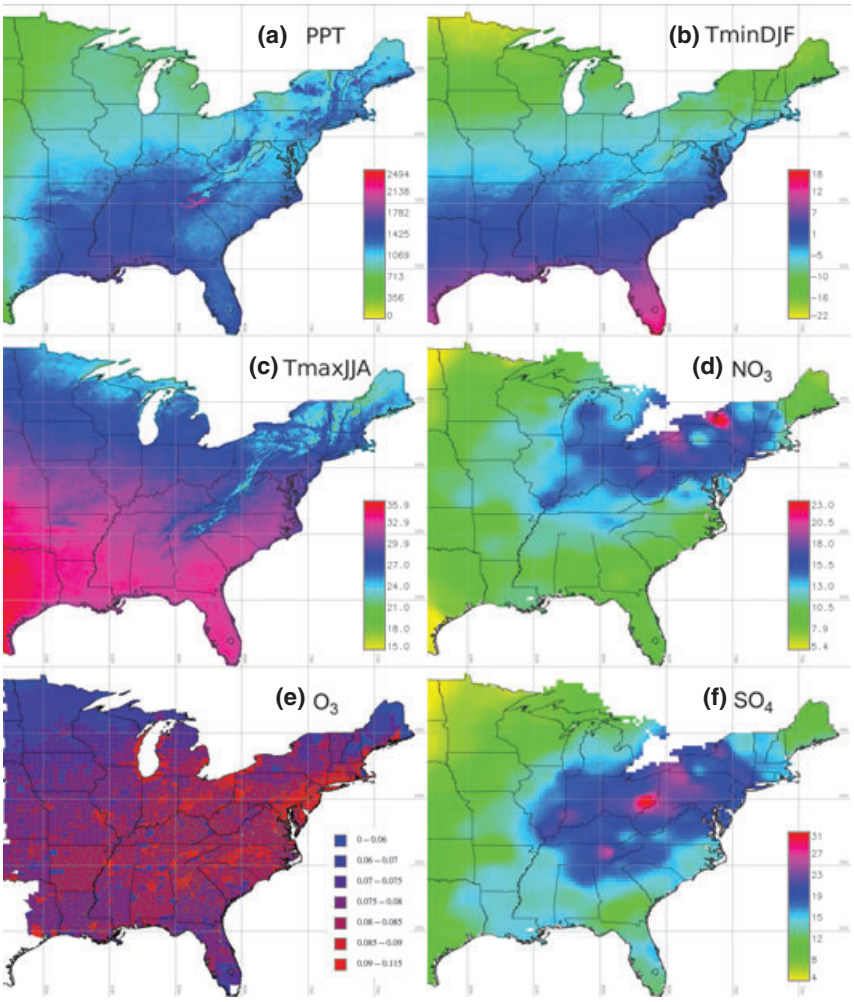

Fig. 2 Regional-scale covariates: (a) mean annual precipitation (mm), (b) mean winter (December–February) minimum temperature (°C), (c) mean summer (June–August) maximum temperature (°C), (d) mean annual nitrate deposition (kg ha^{-1}), (e) mean annual 8 h maximum ozone concentration (ppm), (f) mean annual sulfate deposition (kg ha^{-1}).

hydrogen ion (H^+), and sulfate (SO_4^{2-}) for the period of 1994–2005, based upon readings collected at ca. 200 sampling locations in the study region interpolated onto a ¼ degree resolution grid. Annual maps were then averaged over the study period to estimate the long-term spatial pattern. An initial prescreening showed that for acid deposition the relationship between mortality and sulfate was stronger than for hydrogen ions, while for nitrogen deposition, the relationship between mortality and nitrate was stronger than either ammonium or total nitrogen and thus the analysis considered only nitrate and sulfate. Across the study region, nitrate deposition rates varied from 6 to 16 kg ha^{-1} yr^{-1} while sulfate deposition rates varied from 4 to 30 kg ha yr^{-1}. Nitrate and sulfate are correlated (correlation coefficient of 0.82), with the highest levels of deposition occurring in the Ohio River valley and the northeastern United States (see Fig. 2d and f).

The second source of atmospheric pollutant data was the EPA's AIRDATA database (http://www.epa.gov/oar/data/), which provides annual summary statistics (1996–2006) at the county level for ozone (8 h maximum). The AIRDATA database does not report statistics for every county, so data were averaged over years and interpolated to missing counties using a cokriging model with a spatial polynomial surface for de-trending, human population density as a spatial covariate and a Gaussian autocorrelation function (see Supporting Information for additional details; Banerjee *et al*., 2003). Population density was derived from the US Census Bureau's TIGER database for 2000 (http://www.census.gov/geo/www/tiger/). Across the study region, ozone concentrations varied from 0.050 to 0.114 ppm with highest levels in the mid-Atlantic and a finer-grained spatial pattern concentrated around urban centers (Fig. 2e). The 2008 EPA air quality standard for human health is 0.075 ppm (http://www.epa.gov/ozonedesignations/).

Topographic moisture index

Topographic moisture index was calculated for the study region based on the 1/3 arc-second (ca. 10 m) National Elevation Data DEM (http://seamless.usgs.gov/). The topographic moisture index is defined as

$$\mathrm{TCI} = \ln\left(\frac{a}{\tan(\beta)}\right),$$

where a is upslope flow accumulation area and β is local slope. TCI was derived as part of the TOPMODEL watershed hydrology model and has been shown to correlate closely with differences in soil moisture across the landscape (Beven & Kirby, 1979; Walko *et al*., 2000). As a result of the file size of the DEM (>300 GB), TCI was calculated for 1° tiles using the GRASS package r.terraflow, which implements the TERRAFLOW algorithm of Arge *et al*. (2003). All other topographic covariates were available directly from the FIA database.

Plant functional types

The FIA database contains 267 species in our study region whose abundances vary across almost six orders of magnitude. To reduce complexity, we classified species into 10 plant functional types (PFTs; Table 1) enabled us to maintain the large sample sizes necessary for exploring the effects of multiple drivers of mortality and constrain parameter estimates despite the inherent low frequency of mortality events. To assign trees to PFTs, species were first split into angiosperms and gymnosperms and then were ordered along a successional gradient of shade tolerance from intolerant 'early' species, to intermediate 'mid' species, to shade-tolerant 'late' species. Because of their high abundances and established differences in climatic tolerances, the midsuccessional hardwoods and early successional conifers were each split into a northern and southern group. Two additional groups, evergreen angiosperms and hydric species, were identified as distinct in their autecology from the east temperate forest successional sequence. Hydric species, such as *Taxodium distichum* (Baldcypress), are those that grow in saturated conditions and are particularly tolerant of anoxia. Species assignments to PFT were based primarily upon information from the USDA Plants database (NRCS, 2008), USFS Sylvics Manual (Burns & Honkala, 1990) and Fire Effects Information System (FEIS; http://www.fs.fed.us/database/feis/index.html). The full species list and PFT range maps are given in the Supporting Information.

Statistical model

The analysis of mortality probability (p) is based on the familiar logistic regression model for binary mortality data:

$$\mathrm{logit}(p) = \ln\left(\frac{p}{1-p}\right) = \alpha_0 + \alpha_1 x_1 + \cdots + \alpha_k x_k,$$

where the logit transformation provides the intuitive interpretation of relating changes in the log of the odds ratio to a linear model of the covariates, $\{\mathbf{x}\}$, and regression parameters, $\{\boldsymbol{\alpha}\}$. However, as the re-census interval in the FIA is not annual

Table 1 Plant functional types (PFTs) and major representative species. Full species list and classification can be found in Supporting Information

PFT	Major taxa
Early successional hardwood	*Populus*, *Betula*, *Liquidambar*
Northern midsuccessional hardwood	*Quercus alba*, *Quercus rubra*, *Quercus velutina*
Southern midsuccessional hardwood	*Quercus prinus*, *Quercus stellata*, *Liriodendron*
Late successional hardwood	*Acer*, *Fagus*, *Tilia*
Northern pine	*Pinus strobus*, *Pinus resionosa*, *Pinus banksiana*
Southern pine	*Pinus taeda*, *Pinus elliottii*, *Pinus echinata*
Midsuccessional conifer	*Picea mariana*, *Picea rubens*, *Picea glauca*
Late Successional conifer	*Tsuga*, *Juniperus*, *Abies balsamea*
Evergreen hardwoods	*Magnolia virginiana*, *Quercus virginiana*, *Ilex opaca*
Hydric	*Taxodium*, *Nyssa biflora*, *Nyssa aquatica*

Table 2 Logistic regression model covariates and 95% CI by plant functional type (PFT). Nonsignificant values indicated by ns

		Climate			Pollution		
PFT	Intercept	Precip.	T_{min}	T_{max}	NO_3	SO_4	O_3
Early HW	−10.88 (−7.07, −13.29)	1.49 (1.73, 1.25)	−0.41 (−0.54, −0.26)	1.72 (1.93, 1.46)	0.47 (0.50, 0.45)	−0.24 (−0.23, −0.26)	−22.15 (−16.24, −28.07)
N Mid HW	6.48 (7.20, 5.63)	−0.57 (−0.37, −0.77)	0.19 (0.05, 0.31)	−0.51 (−0.29, −0.68)	−0.08 (−0.07, −0.09)	ns	ns
S Mid HW	−20.43 (−13.95, −25.28)	1.07 (1.28, 0.89)	−0.29 (−0.44, −0.12)	2.41 (2.77, 2.07)	0.69 (0.72, 0.66)	−0.32 (−0.30, −0.33)	−7.66 (−2.81, −12.84)
Late HW	−14.72 (−9.36, −17.39)	0.64 (0.86, 0.44)	−0.16 (−0.30, −0.01)	1.22 (1.46, 0.97)	0.76 (0.79, 0.72)	−0.34 (−0.32, −0.36)	−33.65 (−27.97, −39.09)
N.Pine	15.29 (18.25, 13.35)	−0.41 (0.10, −0.91)	1.53 (1.13, 2.01)	−2.03 (−1.53, −2.73)	0.16 (0.21, 0.10)	−0.14 (−0.10, −0.19)	−45.34 (−27.38, −62.14)
S.Pine	−19.13 (−11.74, −23.15)	1.31 (1.50, 1.12)	−0.65 (−0.45, −0.85)	3.59 (3.92, 2.88)	0.84 (0.88, 0.80)	−0.51 (−0.49, −0.54)	−17.04 (−11.18, −23.55)
Mid Con	10.38 (18.53, 8.10)	1.49 (2.96, −0.14)	ns	ns	0.13 (0.23, 0.04)	ns	ns
Late Con	2.52 (3.15, 1.93)	ns	0.19 (0.10, 0.28)	0.85 (0.98, 0.67)	0.07 (0.08, 0.05)	0.03 (0.04, 0.01)	3.86 (8.39, −0.73)
Evergreen	−19.37 (−11.69, −24.79)	0.81 (1.30, 0.32)	−0.62 (−0.24, −1.01)	5.87 (7.01, 3.85)	1.38 (1.55, 1.21)	−0.62 (−0.51, −0.73)	−71.13 (−54.12, −90.24)
Hydric	−0.05 (1.44, −1.41)	1.39 (1.94, 0.83)	−0.71 (−0.41, −1.01)	ns	0.64 (0.78, 0.49)	−0.14 (−0.05, −0.22)	−17.22 (−1.16, −34.55)

BA, basal area; DBH, diameter at breast height; TCI, topographic moisture index.

and varies at the plot level, we relate annual mortality probability (p_i) of tree i to the observed binomial data on whether that tree lived or died (M_i) via a Bernoulli likelihood,

$$M_i \sim \text{Bern}\left(p_i^{t_i}\right),$$

where t_i is the time interval between successive censuses. Model fitting was performed using Bayesian Markov Chain Monte Carlo (MCMC) methods (Clark, 2007). The prior on $\{\boldsymbol{\alpha}\}$ was set to a diffuse normal distribution for each covariate with mean 0 and standard deviation of 10^4. The analysis was implemented in R (R Development Core Team, 2007) and made extensive use of the R interface with the mySQL database (James & DebRoy, 2007), which was used to store and manipulate the FIA database. The MCMC was implemented using the Metropolis algorithm with a Gaussian jump distribution. Convergence was assessed visually and using the Gelman & Rubin (1992) convergence diagnostic. Chains were run for 50–100K steps, discarding the first 6–20K for burn-in and thinning to 1/3 to reduce autocorrelation. Covariates were initially screened by running each covariate individually, and then running closely correlated variables in pairs (e.g. T_{min} and T_{max}) to verify that including the second provided additional information. Variables were then selected by backward elimination by running the full model and sequentially eliminating covariates whose posterior 95% credible interval was not different from 0. All fits were done independently for each PFT.

As a result of a consistent non-monotonic response in the relationship between mortality and DBH, an additional term was added to the DBH term,

$$\text{D2} = \frac{N(D|a_1, a_2)}{N(a_1|a_1, a_2)},$$

which adds a Gaussian perturbation with mean a_1, standard deviation a_2, and a standardized range between 0 and 1.

Model fit was also assessed using binned plots of the data vs. each covariate individually with mean mortality corrected for census interval and with a 95% credible interval calculated from a beta-binomial posterior with a uniform prior. These plots provide a set of univariate non-parametric mortality functions; however, these mortality curves do not account for the interactions among predictor variables. The fit of the logistic compared with the nonparametric model was assessed in two ways. The first was by generating the 'pure' predicted relationship between each covariate and mortality holding all other covariates at their median value. The second was by predicting the mortality probability of each individual tree accounting for all covariates and then generating binned means for the same bins as the nonparametric model.

Stand						Topography				
Age	BA	DBH	mlc	a_1	a_2	Slope	Rad.	Elev.	TCI	n
0.005 (0.006, 0.004)	−0.21 (−0.18, −0.24)	0.28 (0.35, 0.20)	7.21 (9.61, 4.37)	2.70 (4.33, 1.48)	2.45 (2.60, 2.19)	−0.007 (−0.005, −0.009)	ns	2.05E-4 (2.72E-4, 1.37E-4)	−0.05 (−0.04, −0.06)	78 578
0.002 (0.003, 0.001)	−0.18 (−0.15, −0.20)	0.16 (0.17, 0.16)	2.51 (2.64, 2.39)	3.29 (3.34, 3.24)	0.37 (0.41, 0.33)	−0.003 (−0.002, −0.004)	ns	−1.37E-4 (−8.89E-5, −1.85E-4)	ns	144 168
0.008 (0.009, 0.007)	−0.24 (−0.21, −0.26)	0.34 (0.43, 0.23)	12.21 (16.76, 7.81)	4.17 (6.31, 2.37)	2.74 (2.88, 2.52)	−0.004 (−0.002, −0.006)	0.18 (0.35, 0.00)	2.88E-4 (3.48E-4, 2.28E-4)	−0.05 (−0.04, −0.06)	117 437
0.011 (0.012, 0.009)	−0.22 (−0.19, −0.25)	0.46 (0.54, 0.35)	11.94 (14.57, 7.98)	2.29 (3.74, 1.38)	2.52 (2.62, 2.32)	−0.006 (−0.004, −0.008)	ns	1.37E-4 (1.95E-4, 7.94E-5)	−0.02 (−0.01, −0.04)	78 635
ns	0.06 (0.13, −0.01)	0.08 (0.10, 0.06)	2.07 (3.00, 1.48)	3.67 (3.92, 3.43)	0.02 (0.29, −0.33)	−0.006 (−0.002, −0.010)	ns	−5.63E-4 (−4.49E-4, −6.76E-4)	ns	18 973
−0.013 (−0.011, −0.014)	−0.41 (−0.39, −0.44)	0.57 (0.69, 0.42)	9.35 (12.68, 5.64)	4.12 (5.33, 3.15)	2.14 (2.29, 1.88)	−0.007 (−0.004, −0.009)	ns	−2.49E-4 (−1.83E-4, −3.16E-4)	−0.02 (−0.01, −0.03)	159 476
−0.006 (−0.004, −0.009)	ns	−0.35 (−0.25, −0.67)	−4.60 (−3.06, −10.99)	6.37 (6.82, 4.78)	1.43 (1.98, 1.09)	ns	ns	−6.82E-4 (−3.79E-4, −9.73E-4)	ns	10 620
0.006 (0.007, 0.006)	ns	−0.05 (−0.05, −0.06)	−1.27 (−1.17, −1.41)	7.59 (7.78, 7.40)	1.30 (1.42, 1.19)	0.002 (0.004, 0.000)	−0.43 (−0.18, −0.68)	ns	ns	149 397
0.019 (0.022, 0.016)	−0.15 (−0.07, −0.23)	0.19 (0.26, 0.14)	3.00 (4.45, 2.15)	5.88 (6.55, 5.12)	1.60 (1.89, 1.32)	ns	ns	1.39E-3 (1.97E-3, 8.40E-4)	−0.03 (−0.01, −0.06)	7891
0.021 (0.024, 0.019)	ns	−0.03 (−0.02, −0.04)	−101.9 (−43.24, −243)	−8.78 (−7.20, −10.23)	1.27 (1.40, 1.16)	ns	ns	ns	−0.03 (−0.01, −0.05)	22 352

Finally, the sensitivity of the model covariates were assessed on a covariate × PFT basis. The sensitivity of PFT k to covariate i, $S_{i,k}$, was defined as the standard deviation of the predicted mortality rate for covariate i, $Y_{\mathrm{pred},i}$, holding all other covariates at their mean: $\mathrm{logit}\left(Y_{\mathrm{pred},i}\right) = \beta_{-i}\overline{X_{-i}} + \beta_i X_i$. Sensitivities were multiplied by 1000 to ease comparisons. $S_{i,k}$ can also be calculated for groups of variables to account for the covariance among covariates. The sensitivity of DBH and D2 are calculated together as the overall sensitivity of DBH. The joint sensitivity of NO_3^- and SO_4^{2-} was also calculated because of their high covariance. $S_{i,k}$ provides a common axis for comparison of variables in terms of their affect on the mortality rate. The index is context dependent, in that it assesses variation in the response variable based in part on the observed variability in the independent variable. However, this approach also allows the index to be a global indicator of sensitivity, and thus account for nonlinearities, rather than just a linear approximation around the mean. A number of other sensitivity measures were considered but all gave qualitatively the same results and thus are not shown.

Results

Of the 13 covariates considered, all were significant predictors of tree mortality for more than one of the 10 PFTs, with the frequency of inclusion ranging from 10/10 PFTs for DBH and NO_3^-, to 2/10 PFTs for the topographic radiation index (Table 2, Fig. 3). Among the climate variables, mortality decreases with increased precipitation as hypothesized for 7/10 of PFTs but increases for the two northern PFTs and is not significant for late successional conifers. For minimum winter temperature, only three PFTs conformed to our original hypothesis of increased mortality in colder winters (NMH, NP, LC) while six PFTs increased mortality for warmer winters. By contrast, six PFTs conformed to our expected decline in mortality with warm summers while only the two northern PFTs showed increased mortality with warm summers. The most consistent results were seen among atmospheric pollutants. For nitrogen deposition, nine PFTs conformed to our expectation of decreased mortality with increased nitrogen deposition, with only NMH showing the opposite pattern. For acid deposition, seven PFTs showed large increases in mortality with deposition and only one (late successional conifers) showed a weak decline. Of the eight PFTs showing a significant relationship with ozone, there was a

unanimous increase in mortality with increasing ozone concentration.

The effects of landscape-scale heterogeneity were comparatively weaker. Eight PFTs showed a correlation with elevation, but these were evenly split between increases and decreases in mortality. The only consistent trend was an increase in mortality with elevation for the conifer species and a decline in mortality with elevation for 4/5 of the hardwoods. The effects of slope generally conformed to the expected increase in mortality with increased slope (6 increasing vs. 1 decreasing). The topographic radiation index was not significant for eight of 10 PFTs and was inconsistent for the remaining two, showing an increase in mortality on southern exposures for LC and a decrease for SMH. On the other hand, the topographic moisture index was significant for 6/10 of the PFTs and showed a consistent increase in mortality for the wettest landscape positions. At the stands scale, there was a clear relationship between DBH and mortality for all taxa, but the relationship was nonlinear (Fig. 3) and only conformed to the expected J-shaped curve for only one PFT (Hydric). Of the remaining PFTs, two were missing a clear signal of elevated juvenile mortality and all showed clear evidence for a midlife increase in mortality rate. The general mortality–size relationship is thus closer to a W than a J. For all PFTs, there were insufficient data to place a clear constraint on the senescent phase. For stand basal area, there was a generally consistent trend of increased mortality in older stands (6 increasing, 1 weakly decreasing, 3 ns). Finally, for stand age, six PFTs showed a decline in mortality rates in older stands while only two (SP, MC) showed an increase in mortality with age.

Sensitivity scores

The covariates spanned a wide range of sensitivities, but clear overall trends emerge (Table 3). Calculating the mean sensitivity by covariate and by PFT shows that overall tree mortality was most sensitive to atmospheric pollutants, with acid deposition showing the highest sensitivity and nitrogen deposition coming in third and ozone was ranked ninth of the 13 covariates. Even after accounting for the high covariance between N and acid deposition (N × S), the combined effect still shows one of the highest sensitivities. Stand-scale biotic factors showed the second highest sensitivities, largely driven by the effects of individual-tree size (DBH), which was the second most important variable overall. Stand age also ranked near the top at fifth, while basal area (10th) came in at the low end of the middle group. Regional-scale climatic variables were the next most important group of covariates, with summer temperature showing the fourth highest sensitivity, and precipitation and winter temperature being in the middle group. Landscape-level topographic effects had the weakest effect on tree mortality, with elevation being in the middle group while topographic moisture, slope, and topographic radiation rounded out the bottom.

When examined on a PFT basis, evergreen hardwoods were clearly the group that was most sensitive to their environment. By contrast, northern midsuccessional hardwoods and mid and late successional conifers showed an overall low sensitivity. There was no correlation between sample size and species sensitivities ($P > 0.05$, $F = 0.408$), which holds even if evergreen hardwoods (relatively low sample size, high sensitivity) is removed.

Discussion

The most striking result of this analysis is the unexpectedly large role of atmospheric pollutants on the mortality rates of eastern forests (Figs 2 and 3). This is in contrast to the work by van Mantgem *et al.* (2009) that ruled out a strong role of atmospheric pollutants on western forests. The strongest effect appears to be due to the effects of long-term acidification, particularly in the northeast. The lack of a significant acid deposition effect on midsuccessional conifers (predominantly spruces and firs), the group of trees with the most well known and documented response to acidification (DeHayes *et al.*, 1999; Tomlinson, 2003), should not be taken as a refutation of previous stand-level work, but rather suggests there is reason for concern about the other taxa that have received comparatively less attention. For example, despite the fact that acidification is considered primarily a northeastern problem (Driscoll *et al.*, 2001; Tomlinson, 2003), with some evidence for declines among high-elevation southern spruce/fir stands (McLaughlin *et al.*, 1994), there are also significant negative impacts among predominantly southern PFTs (southern midsuccessional hardwoods, southern pines, evergreen hardwoods, and hydric).

By contrast, the impacts of nitrogen deposition were almost as strong, but caused a decline in mortality, suggesting that the fertilization effects of NO_3^- are currently stronger than the negative impacts of acidification of NO_3^-. While not captured by the fitted model, there is some suggestion that at very high levels of deposition mortality begins to increase again (full set of covariate by PFT plots provided in Supporting Information). Contrary to the expectation, sensitivity to nitrogen deposition does not appear to vary systematically with shade tolerance, although

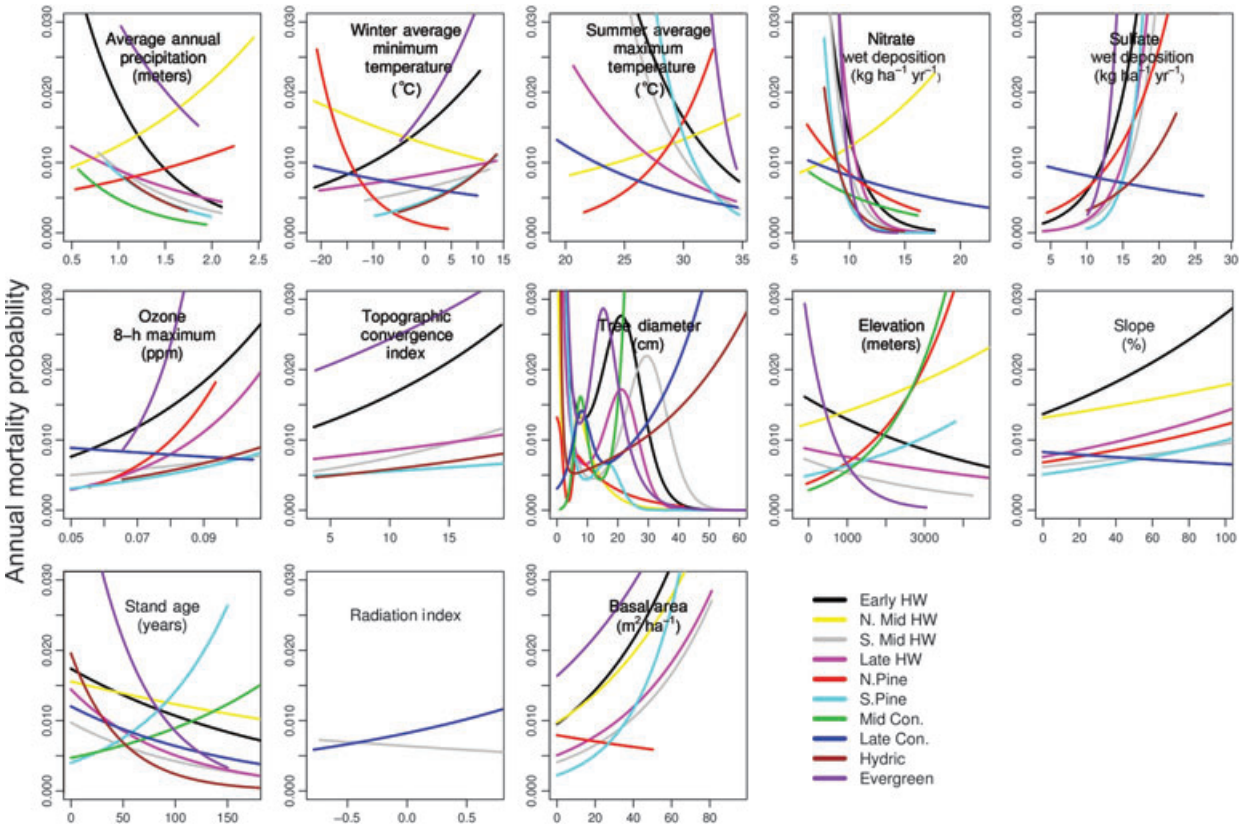

Fig. 3 Mean effects of each driver by plant functional type. Only significant results are shown. The variable on the *x*-axis is given in the title of each panel with the units in parenthesis. Some covariates are dimensionless.

Table 3 Parameter sensitivities: mortality rates show the highest sensitivities to stem diameter, SO_4 and NO_3 deposition, and summer maximum temperature. The joint sensitivity of mortality to NO_3 and SO_4, N × S, remains high despite the high covariance between the two variables. Overall, sensitivities to landscape-scale topographic variables were low

	Climate			Pollution				Stand			Topography				
PFT	Precip	T_{min}	T_{max}	NO_3	SO_4	N × S	O_3	Age	BA	DBH	Slope	Rad	Elev	TCI	Mean
Early HW	7.70	3.97	13.34	12.99	21.46	7.48	2.37	1.52	2.50	9.40	1.37	ns	1.56	1.97	6.1651
N Mid HW	1.82	1.56	1.63	2.02	ns	ns	ns	ns	1.97	6.00	0.71	ns	1.07	ns	1.3501
S Mid HW	1.08	0.58	4.28	8.44	20.52	4.76	0.23	1.25	1.21	13.55	0.46	0.15	0.87	0.77	4.0948
Late HW	1.50	0.83	3.71	18.18	38.02	9.19	1.78	2.08	1.50	14.42	0.93	ns	0.65	0.49	6.4682
N.Pine	0.79	6.31	3.18	2.78	8.25	5.74	2.71	ns	0.36	1.87	0.74	ns	2.79	ns	2.2916
S.Pine	0.91	0.77	3.52	5.54	42.48	4.06	0.37	1.59	1.87	29.56	0.36	ns	0.48	0.27	6.747
Mid Con	0.92	ns	ns	1.17	ns	ns	ns	1.38	ns	5.98	ns	ns	8.55	ns	1.3839
Late Con	ns	0.91	1.59	1.20	1.00	1.99	0.26	1.64	ns	3.78	0.22	0.35	ns	ns	0.8157
Evergreen	2.48	3.37	19.19	31.81	52.42	9.82	7.22	10.70	3.17	28.66	ns	ns	3.52	2.19	12.672
Hydric	1.05	0.99	ns	4.74	1.08	2.79	0.38	3.40	ns	24.92	ns	ns	ns	0.54	2.8529
Mean	1.82	1.93	5.04	8.89	18.52	4.58	1.53	2.43	1.26	13.81	0.48	0.05	1.95	0.62	

PFT, plant functional type; BA, basal area; DBH, diameter at breast height; TCI, topographic moisture index.

hardwoods do appear to be slightly more sensitive than conifers (average sensitivity 14.7 vs. 2.7). This trend contrasts with the finding at the nitrogen saturation experiment at Harvard Forest, which saw a larger response from pines than among hardwoods (Magill *et al.*, 2004).

The impacts of both acidification and nitrogen deposition on tree mortality result from cumulative, long-term deposition, and the patterns presented here should be interpreted in that light – these relationships are not intended to assess the impacts of interannual variability in deposition nor the efficacy of NO_3^- or SO_4^{2-} regulation. Still, despite a 36% decline in SO_4^{2-} deposition from 1990 to 2005 (US EPA, 2008), evidence suggests that the problem of acid rain is ongoing and forest soils are continuing to see declines in base cations (G. Likens, personal communication).

The impacts of ozone were consistently negative as hypothesized and as expected angiosperms were more sensitive to ozone than conifers (average sensitivity of 2.3 vs. 0.8). The differences in mortality rates among functional types conforms roughly to the differences in the impact of ozone on growth rates found in a recent meta-analysis (Wittig *et al*., 2007), which themselves follow the different patterns of stomatal conductance among species. It is not surprising that the impacts of ozone on mortality map well to differences in stomatal conductance because the main impacts of ozone are due to the long-term oxidative damage occurring in the leaf intercellular spaces and thus is well modeled by the cumulative ozone uptake through the leaf stomata (Reich, 1987). Our estimates of ozone impacts are likely underestimated for three reasons. First, ozone concentrations were only observed in about half the counties and thus had to be inferred in the remaining areas. This is problematic because ozone is relatively short lived in the atmosphere, showing a finer scale spatial pattern than NO_3^- or SO_4^{2-}, and thus interpolation errors are likely to be higher. Second, our interpolation scheme that sought to account for production, via population density, did not account for the dominant wind directions of transport nor differences in ozone destruction due to reactions with hydrocarbon compounds. Third, we used the peak 8 h ozone concentrations as our ozone estimate as this is the basis of current health standards and regulation. This is potentially problematic because plants, unlike animals, are more sensitive to cumulative exposure rather than peak exposure. Still, peak and cumulative concentrations are highly correlated (figure not shown) and we expect our conclusions regarding the effects of ozone to be qualitatively robust.

Stand-level biotic factors as a group had the second strongest impact on mortality led by the strong effect of individual-tree DBH. As in previous studies (Vieilledent *et al*., 2009, 2010), a clear DBH signal is seen (Fig. 3); however, the functional response proves to be more complicated than the traditional J-shaped mortality function in which mortality is high among juveniles, low for adults, and slowly elevates again in large size classes over time due to senescence. Instead we find a pronounced 'midlife crisis' among most taxa, where there exists an intermediate stage in which mortality rates are significantly elevated.

Below we propose a simple conceptual model that suggests this W-shaped relationship between diameter and mortality is likely to arise from three well-established processes (Fig. 4). The first relationship is that between tree size and growth rate whereby growth is generally assumed to be low among juveniles, to peak at intermediate sizes, and then decline among large trees as senescence begins (Fig. 4a). The second relationship is that between tree growth rate and mortality rate, which is decreasing and roughly exponential in shape (Fig. 4b). These two curves put together predict the classic J-shaped mortality curve (Fig. 4d, dashed line). We hypothesize that the intermediate peak arises due to self-thinning (Fig. 4c). The 3/2 thinning curve (Yoda *et al*., 1963) sets an upper limit to the relationship between stem density and stand biomass due to light competition during canopy closure (Fig. 4c, dashed line). The trajectory of a population through time starts on the bottom of this graph where densities are high and the average biomass per individual is low. Over

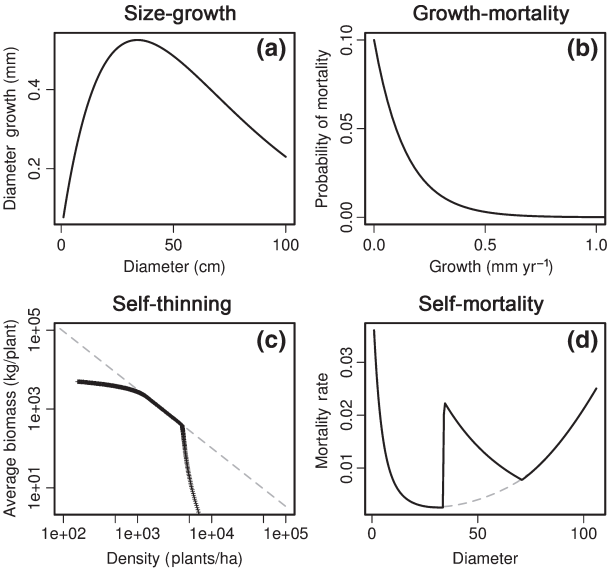

Fig. 4 Conceptual model of the W-shaped relationship between tree size and mortality. The relationships between tree size and growth (a) and tree growth and mortality (b) together predict the classic J-shaped relationship between size and mortality (d, dashed line). The inclusion of a self-thinning phase (c, dashed line) can produce the intermediate-sized increase in mortality rates (d, solid line). The overall population trajectory begins in the lower right with small plants at high density and proceeds upward until canopy closure (inflection point) at which point mortality is driven by thinning until, during the senescence phase (top left), growth declines cause an increase in mortality and the canopy begins to open up again.

time biomass increases and population density declines somewhat, due to juvenile mortality, causing a mostly vertical trajectory until canopy closure, at which time there is an inflection point and densities begin to decline more rapidly, causing the intermediate mortality peak. As growth rates begin to decline so does the rate at which we move along the thinning curve and thus mortality rates decline. Eventually as senescence progresses growth declines to the point that mortality rates begin to increase again, the population leaves the thinning curve, and the canopy begins to open up again. This hypothesized series of events maps well onto the forest developmental stages of 'stand initiation', 'stem exclusion', and 'understory re-initiation' (Oliver and Larson, 1996).

This conceptual model for the W-shaped mortality curve is supported by the differences in peak location and prominence among PFTs, which tends to be earlier and larger in early successional species, especially pines. The lack of a juvenile peak in some of the PFTs is not particularly surprising because the FIA's lower size limit for censuses is fairly large and it is likely that the peak for these PFTs is below the size threshold. This argument is corroborated by studies of seedling survivorship (e.g. Ibáñez *et al*., 2008) that show mortality rates much higher than those we observed here for adults. The weak relationships in the senescent phase are also not surprising due to the smaller sample size in the large size classes. However, the differences among PFTs in the size at onset of senescence is consistent with traditional shade-tolerance rankings (Burns & Honkala, 1990), with earlier successional species showing an earlier and stronger response. The causes of senescence are multifaceted and our results do not distinguish among the various hypotheses, such as mechanical limits on tree size (King, 1990), hydrologic stress (Ryan & Yoder, 1997; Koch *et al*., 2004), metabolic stress due to the differences in scaling between respiration and photosynthesis (Yoda *et al*., 1965) and accumulated crown damage and fungal rot (Pelt & Sillett, 2008).

The effects of stand age on survival varied between conifers and hardwoods. For conifers, we observed a strong increase in mortality rates with age in the southern pine PFT and a transition of declining sensitivities across the successional spectrum that conforms to our initial hypothesis. By contrast, for deciduous angiosperms, we see a decline in mortality with stand age across all functional types that does not vary with successional status, while for evergreen angiosperms, we see the highest sensitivity and high mortality rates in young stands. Overall mortality increased with basal area as expected, with six of seven significant relationships following this trend and the one contrasting PFT (northern pines) which showed the lowest sensitivity is barely statistically significant. Moreover, as predicted, the sensitivity to basal area decreased from the early successional groups to the late successional groups, but what was not predicted was that hardwoods were on average four times more sensitive to stand basal area than conifers.

As a category, the effects of climate were a surprising third place in terms of average sensitivity. Among the climate variables, mean summer maximum temperature had the strongest impact, ranking fourth overall. As predicted, mortality declined with increasing temperature for six of eight PFTs, potentially due to longer growing seasons and higher NPP. Not surprisingly, evergreen hardwoods had the highest sensitivity to summer temperature. Interestingly, the two contrasting PFTs that showed increases in mortality with summer temperature were the two northern groups (northern pines and northern midsuccessional hardwoods). Neither group showed a sharp increase in mortality at their southern range limit, but rather a general increase in mortality across the range of summer temperatures, but these results are consistent with rising mortality rates being associated with southern range limits. The general trend of decreasing mortality with temperature found here for eastern species contrasts with the findings of van Mantgem *et al*. (2009), who observed a regional-scale increase in tree mortality rates in western United States that they attributed to rising temperatures and increasing drought index. Several factors may account for the difference. First, drought stress is comparatively more common in western forests. Second, the current analysis focuses on gradients across space rather than through time and thus, as mentioned above, the current relationships do not necessarily hold for attributing interannual variability. Third, both ecotypic variation within species and acclimation within individuals can make species more vulnerable to climatic change in place than to differences across their range (e.g. Oleksyn *et al*., 1998).

For winter mean minimum temperature, we find a more ambiguous split between five PFTs that show a decrease in mortality with colder winters while three show an increase with colder winter temperatures. Of the three PFTs in which mortality declines in the cold, two are the northern PFTs (northern pine and northern midsuccessional hardwood) that also had a contrasting response to summer temperature while the third is the late successional conifers, which also tends to grow further north than average. The majority trend of increasing mortality with warm winters is consistent with our hypothesis of an indirect effect due to the overwinter survival of pests and pathogens. Indeed, forest pathogens are expected to increase with warming (Kliejunas *et al*., 2009) and a number of recent insect

outbreaks have been attributed in part to increased overwinter survival (Allen *et al*., 2010). Counter to what we hypothesized, the southern PFTs showed lower sensitivity to winter temperature than their northern counterparts. The higher sensitivity and opposite mortality response among the northern PFTs is likely to reflect direct effects of winter cold, such as ice damage or freeze embolism.

Of the climate variables, mortality was least sensitive to mean annual precipitation. Responses were generally consistent with our overall prediction, with seven PFTs showing decreased mortality with increases in precipitation and the two PFTs with the positive responses again being the two northern PFTs. Counter to our expectation of higher sensitivities among hardwoods and among late successional species, there are no clear trends among PFTs. In contrast to our findings, Condit *et al*. (2004) found that across a moisture gradient in Panama, mortality increased with moisture for normal years, but that only the driest site had elevated mortality during an El Niño year. van Mantgem *et al*. (2009) found no direct response to precipitation in western forests but did find a response to drought index. The 6-year Throughfall Displacement Experiment (TDE) in the moist temperate forests of Oak Ridge, TN showed that changes in precipitation by ±33% did not have a significant impact on adult trees but that sapling mortality rates were elevated in the dry plot especially during drought years (Hanson *et al*., 2001). By contrast, the Amazonian TDE in Tapajos, Brazil found significant increases in adult mortality with precipitation reduction but considerably smaller impacts on saplings (Nepstad *et al*., 2007). Numerous studies have provided clear documentation of drought-induced mortality (Allen *et al*., 2010), but overall our results suggest that Eastern temperate trees may be less sensitive to average precipitation than to interannual variability in precipitation.

Landscape-scale topographic variability had surprisingly small impacts on tree mortality rates. The strongest landscape-scale effect was from elevation where, counter to our hypothesized increase in mortality, PFTs were split evenly between four increasing and four decreasing. Conifers were consistently negative and generally more sensitive to elevation than the hardwoods, which generally responded positively but with low sensitivity. For the topographic moisture index, effects were generally weak but, counter to expectation, all six PFTs that had a significant effect showed a consistent increase with increasing soil moisture. As overall precipitation patterns were already accounted for, this effect may be a rooting depth effect, an anoxia effect, or an indirect effect, such as an increase in pathogens or competition. The effects of hillslope, on the other hand, were consistent with predictions, with six species increasing mortality with slope and only late conifers decreasing, and that effect had the lowest sensitivity and was barely significant. Finally, the effects of the solar radiation index, which is primarily a reflection of aspect but also accounts for differences in slope, were inconsistent and had by far the lowest overall sensitivities.

In evaluating the relative sensitivity of tree mortality to environmental drivers, it is important to put these in the context of the overall trends. As a whole, eastern temperate forests are still recovering from the land-use legacy of 18th century agriculture and logging and thus mean DBH, stand age, and basal area are all increasing. Based on these results, it is likely that mortality rates due to competitive and successional processes will increase in the future. Of all the atmospheric pollutants considered, SO_4^{2-} may have the strongest effect but it is also the most regulated, and thus has been declining steadily since the passage of the Clean Air Act (US EPA, 2008). However, overall soil acidification is still increasing and thus mortality rates are likewise expected to continue to increase. Nitrogen deposition and O_3, by contrast, are both projected to rise (Galloway *et al*., 2004; Fowler, 2008) and thus mortality rates are likely to become increasingly sensitive. By contrast, the effects of landscape-scale topographic variability are generally weak and remain fixed on ecological time scales. Viewed in this overall context, it is clear that to anticipate the effects of climate change on tree mortality directly, and forest dynamics in general, will require that we account for multiple interacting global change factors. It is also clear that, of the factors considered in this analysis, climate is subject to the greatest interannual variability. Thus, while acknowledging the previous caveat about not being able to directly infer the effects of variability in time from the effects of spatial variability, it is nonetheless likely that changes in tree mortality rates due to gradual changes in mean climate will have significant, but not severe, direct effects on the mortality of established adult trees. Of much greater concern are the potential effects of climate extremes on adult tree mortality and understory recruitment and survival.

This analysis was designed to understand the relative strengths of different drivers of tree mortality. The impacts of each factor was typically consistent with expectations and while there are a number of trends that will require further investigation and clarification, the overall strength of atmospheric pollutants was surprising. Critical next steps include the need to separate out the effects of individual mortality agents and to separate out the dynamics of individual species to better understand the drivers of variability in mortality

(e.g. different life history traits or phylogenetic constraints). Also essential, but considerably more difficult with the available data, is to differentiate the effects of spatial and temporal variability in mortality and in particular to distinguish the responses to average conditions presented here from the responses to interannual variability in climate and pollutants, which may be much more relevant to short-term global change responses. Nonetheless, what is ultimately lacking is a coherent, physiologically based theory of tree mortality (McDowell *et al*., 2008). Such an approach will be necessary to unify the disparate effects of numerous covariates in terms of a single quantitative measure of tree stress and to model how novel environmental conditions will affect tree survival, forest dynamics, and the terrestrial carbon cycle.

Acknowledgements

Funding was provided by DOE NICCR grant DE-FC02-06ER64157 to Paul Moorcroft. We thank Liz LaPoint at the USFS FIA Spatial Data Center for assistance in extracting topographic moisture and soils data layers. We thank Dan Lipsitt for assistance in downloading and processing topographic data. We also thank David LeBauer, Dan Wang, Xiaohui Feng, Jim Clark, Jeff Herrick, Jessica Metcalf, and Victoria Witting for useful discussions and comments.

References

Allen CD, Mackalady AK, Chenchouni H *et al*. (2010) A global overview of drought and heat-induced tree mortality reveals emerging climate change risks for forests. *Forest Ecology and Management*, **259**, 660–684.

Arge L, Chase J, Halpin P, Toma L, Urban DL, Vitter JS, Wickremesinghe R (2003) Efficient flow computation on massive grid terrains datasets. *Geoinformatica*, **7**, 283–313.

Baldocchi D (2008) 'Breathing' of the terrestrial biosphere: lessons learned from a global network of carbon dioxide flux measurement systems. *Australian Journal of Botany*, **56**, 1–26.

Banerjee S, Carlin B, Gelfand A (2003) *Hierarchical Modeling and Analysis for Spatial Data*. Chapman & Hall/CRC, London. ISBN: 978-1584884101.

Beven KJ, Kirby MJ (1979) A physically based, variable contributing area model of basin hydrology. *Hydrological Sciences Bulletin*, **24**, 43–69.

Breshears DD, Cobb NS, Rich PM *et al*. (2005) Regional vegetation die-off in response to global-change-type drought. *Proceedings of the National Academy of Sciences, USA*, **102**, 15144–15148.

Brown SL, Schroeder PE (1999) Spatial patterns of aboveground production and mortality of woody biomass for eastern U.S. forests. *Ecological Applications*, **9**, 968–980.

Burns RM, Honkala BH (1990) *Silvics of North America: 1. Conifers; 2. Hardwoods*. Agriculture Handbook 654, Vol. 2. U.S. Department of Agriculture, Forest Service, Washington, DC.

Caswell H (2001) *Matrix Population Models* (2nd edn). Sinauer Associates, Sunderland, MA.

Clark JS (2007) *Models for Ecological Data: An Introduction*. Princeton University Press, Princeton, NJ.

Condit R, Aguilar S, Hernandez A *et al*. (2004) Tropical forest dynamics across a rainfall gradient and the impace of and El Nino dry season. *Jounal of Tropical Ecology*, **20**, 51–72.

Daly C, Halbleib M, Smith JI *et al*. (2008) Physiographically-sensitive mapping of temperature and precipitation across the conterminous United States. *International Journal of Climatology*, **28**, 2031–2046.

DeHayes D, Schaberg P, Hawley G, Strimbeck G (1999) Acid rain impacts on calcium nutrition and forest health. *BioScience*, **49**, 789–800.

Driscoll CT, Lawrence GB, Bulger AJ *et al*. (2001) Acidic deposition in the northeastern United States: sources and inputs, ecosystem effects, and management strategies. *BioScience*, **51**, 180–198.

Eid T, Tuhus E (2001) Models for individual tree mortality in Norway. *Forest Ecology and Management*, **154**, 69–84.

Elliott KJ, Swank WT (1994) Impacts of drought on tree mortality and basal area growth in a mixed hardwood forest of the Coweeta Basin. *Journal of Vegetation Science*, **5**, 229–236.

Food and Agriculture Organization (FAO) of the United Nations (2007) *State of the World's Forests 2007*. FAO, Rome.

Fowler D (2008) *Ground-Level Ozone in the 21st Century: Future Trends, Impacts and Policy Implications*. Royal Society, London, UK.

Franco M, Silvertown J (1996) Life history variation in plants: an exploration of the fast-slow continuum hypothesis. *Philosophical Transactions of the Royal Society B: Biological Sciences*, **351**, 1341–1348.

Fridman J, Stahl G (2001) A three-step approach for modeling tree mortality in Swedish forests. *Scandinavian Journal of Forest Research*, **16**, 455–466.

Galloway JN, Dentener FJ, Capone DG *et al*. (2004) Nitrogen cycles: past, present, and future. *Biogeochemistry*, **70**, 153–226.

Gelman A, Rubin DB (1992) Inference from iterative simulation using multiple sequences. *Statistical Science*, **7**, 457–511.

Gholz HL, Wedin DA, Smitherman SM, Harmon ME, Parton WJ (2000) Long-term dynamics of pine and hardwood litter in contrasting environments: toward a global model of decomposition. *Global Change Biology*, **6**, 751–765.

GRASS Development Team (2007) *GRASS 6.2 Users Manual*. ITC-irst, Trento, Italy. Available at: http://grass.osgeo.org/grass62/manuals/html62_user/ (accessed 28 February 2011).

Hanson PJ, Todd DE, Amthor JS (2001) A six-year study of sapling and large-tree growth and mortality responses to natural and induced variability in precipitation and throughfall. *Tree physiology*, **21**, 345–358.

Holdridge LR (1967) *Life Zone Ecology*. Tropical Science Center, San Jose, Costa Rica.

Ibáñez I, Clark JS, Dietze MC (2008) Evaluating the sources of potential migrant species: implications under climate change. *Ecological Applications: A Publication of the Ecological Society of America*, **18**, 1664–1678.

James DA, DebRoy S (2007) *RMySQL: R Interface to the MySQL Database*. R package version 0.6-0. Available at: http://cran.r-project.org/web/packages/RMySQL/ (accessed 8 July 2008).

Keane R, Austin M, Field C *et al*. (2001) Tree mortality in gap models: application to climate change. *Climatic Change*, **51**, 509–540.

King DA (1990) The adaptive significance of tree height. *The American Naturalist*, **135**, 809–828.

King AW, Post WM, Wullschleger SD (1997) The potential response of terrestrial carbon storage to changes in climate and atmospheric CO_2. *Climatic Change*, **35**, 199–227.

Kliejunas J, Geils B, Glaeser J *et al*. (2009) *Review of literature on climate change and forest diseases of western North America*. USFS General Technical Report PSW-GTR-225, USFS Albany, CA.

Kobe RK (1996) Intraspecific variation in sapling mortality and growth predicts geographic variation in forest composition. *Ecological Monographs*, **66**, 181–201.

Kobe RK, Likens GE, Eagar C (2002) Tree seedling growth and mortality responses to manipulations of calcium and aluminium in a northern hardwood forest. *Canadian Journal of Forest Research*, **32**, 954–966.

Koch GW, Sillett SC, Jennings GM, Davis SD (2004) The limits to tree height. *Nature*, **428**, 851–854.

Köppen W (1931) *Grundriss der klimakunde*. Walter de Grwyter, Berlin.

Körner C (2007) The use of 'altitude' in ecological research. *Trends in Ecology and Evolution*, **22**, 569–574.

Magill AH, Aber JD, Currie WS *et al*. (2004) Ecosystem response to 15 years of chronic nitrogen additions at the Harvard Forest LTER, Massachusetts, USA. *Forest Ecology and Management*, **196**, 7–28.

Maherali H, Pockman WT, Jackson RB (2004) Adaptive variation in the vulnerability of woody plants to xylem cavitation. *Ecology*, **85**, 2184–2199.

van Mantgem PJ, Stephenson NL, Byrne JC *et al*. (2009) Widespread increase of tree mortality rates in the western United States. *Science*, **323**, 521–524.

McDowell N, Pockman WT, Allen C *et al*. (2008) Mechanisms of plant survival and mortality during drought: why do some plants survive while others succumb to drought? *New Phytologist*, **178**, 719–739.

McLaughlin SB, Joslin JD, Stone A, Wimmer R, Wullschleger S (1994) *Effects of Acid deposition on Calcium Nutrition and Health of Southern Appalachian Spruce Fir Forests*. International Union of Forest Resource Organizations (IUFRO) Conference, New Brunswick, Canada.

Monserud RA, Sterba H (1999) Modeling individual tree motaltiy for Austrian forest species. *Forest Ecology and Management*, **113**, 109–123.

Moorcroft PR, Hurtt GC, Pacala SW (2001) A method for scaling vegetation dynamics: the ecosystem demography model (ED). *Ecological Monographs*, **71**, 557–586.

Nepstad DC, Tohver IM, Ray D, Moutinho P, Cardinot G (2007) Mortality of large trees and lianas following experimental drought in an Amazon forest. *Ecology*, **88**, 2259–2269.

NRCS (2008) *The PLANTS Database*. National Plant Data Center, Baton Rouge, LA, USA. Available at: http://plants.usda.gov.

Oleksyn J, Tjoelker MG, Karolewski P (1998) Growth and physiology of Picea abies populations from elevational transects: common garden evidence for altitudinal ecotypes and cold adaptation. *Functional Ecology*, **12**, 573–590.

Oliver CD, Larson BC (1996). *Forest Stand Dynamics*. John Wiley & Sons Inc., New York, NY. ISBN: 978-0471138334.

Pacala S, Canham C, Saponara J, Silander J, Kobe R, Ribbens E (1996) Forest models defined by field measurements: estimation, error analysis and dynamics. *Ecological Monographs*, **66**, 1–43.

Pelt R, Sillett S (2008) Crown development of coastal Pseudotsuga menziesii, including a conceptual model for tall conifers. *Ecological Monographs*, **78**, 283–311.

Phillips OL, Baker TR, Arroyo L *et al*. (2004) Pattern and process in Amazon tree turnover, 1976–2001. *Philosophical Transactions of the Royal Society B: Biological Sciences*, **359**, 381–407.

R Development Core Team (2007) *R: A Language and Environment for Statistical Computing*. R Foundation for Statistical Computing, Vienna, Austria. ISBN: 3-900051-07-0. Available at: http://www.R-project.org.

Reich PB (1987) Quantifying plant response to ozone: a unifying theory. *Tree Physiology*, **3**, 63–91.

Running SW, Nemani RR, Heinsch FA, Zhao M, Reeves M, Hashiomoto H (2004) A continuous satellite-derived measure of global terrestrial primary production. *BioScience*, **54**, 547–560.

Ryan M, Yoder B (1997) Hydraulic limits to tree height and tree growth. *BioScience*, **47**, 235–242.

Shifley SR, Fan Z, Kabrick JM, Jensen RC (2006) Oak mortality risk factors and mortality estimation. *Forest Ecology and Management*, **229**, 16–26.

Shinano T, Osaki M, Kato M (2001) Differences in nitrogen economy of temperate trees. *Tree Physiology*, **21**, 617–624.

Smith B, Prentice IC, Sykes MT (2001) Representation of vegetation dynamics in the modelling of terrestrial ecosystems: comparing two contrasting approaches within European climate space. *Global Ecology and Biogeography*, **10**, 621–638.

Smith WB, Miles PD, Vissage JS, Pugh SA (2002) *Forest resources of the United States, 2002*. General Technical Report NC-241, USDA North Central Forest Experiment Station, St. Paul, MN.

Sperry JS, Sullivan JE (1992) Xylem embolism in response to freeze-thaw cycles and water stress in ring-porous, diffuse-porous, and conifer species. *Plant Physiology*, **100**, 605–613.

Sperry J, Hacke U, Pittermann J (2006) Size and function in conifer tracheids and angiosperm vessels. *American Journal of Botany*, **93**, 1490.

Thornton P, Law BE, Gholz HL *et al*. (2002) Modeling and measuring the effects of disturbance history and climate on carbon and water budgets in evergreen needleleaf forests, *Agricultural and Forest Meteorology*, **113**, 185–222.

Tomlinson GH (2003) Acid deposition, nutrient leaching and forest growth. *Biogeochemistry*, **65**, 51–81.

U.S. Environmental Protection Agency (EPA) (2008) *EPA's 2008 Report on the Environment*. National Center for Environmental Assessment, Washington, DC; EPA/600/R-07/045F. National Technical Information Service, Springfield, VA. Available at: http://www.epa.gov/roe.

Vieilledent G, Courbaud B, Kunstler G, Dhote J, Clark JS (2009) Biases in the estimation of size-dependent mortality models: advantages of a semiparametric approach. *Canadian Journal of Forest Research*, **39**, 1430–1443.

Vieilledent G, Courbaud B, Kunstler G, Dhôte J (2010) Mortality of silver fir and Norway Spruce in the Western Alps – a semi-parametric approach combining size-dependent and growth-dependent mortality. *Annals of Forest Science*, **67**, 305.

Walko RL, Band LE, Baron J *et al*. (2000) Coupled atmosphere–biophysics–hydrology models for environmental modeling. *Journal of Applied Meteorology*, **39**, 931–944.

Whittaker RH (1956) Vegetation of the Great Smoky Mountains. *Ecological Monographs*, **26**, 2–80.

Wittig VE, Ainsworth EA, Long SP (2007) To what extent do current and projected increases in surface ozone affect photosynthesis and stomatal conductance of trees? A meta-analytic review of the last 3 decades of experiments. *Plant, Cell and Environment*, **30**, 1150–1162.

Woodall CW, Grambsch PL, Thomas W (2005a) Applying survival analysis to a large-scale forest inventory for assessment of tree mortality in Minnesota. *Ecological Modelling*, **189**, 199–208.

Woodall CW, Grambsch PL, Thomas W (2005b) Survival analysis for a large-scale forest health issue: Missouri oak decline. *Environmental Monitoring and Assessment*, **108**, 295–307.

Wright IJ, Reich PB, Westoby M *et al*. (2004) The worldwide leaf economics spectrum. *Nature*, **428**, 821–827.

Wyckoff P, Clark J (2000) Predicting tree mortality from diameter growth: a comparison of maximum likelihood and Bayesian approaches. *Canadian Journal of Forest Research*, **30**, 156–167.

Yoda K, Kira T, Ogawa H, Hozumi K (1963) Self-thinning in overcrowded pure stands under cultivated and natural conditions (Intraspecific competition among higher plants XI). *Journal of the Institute of Polytechnics, Osaka City University, Series D*, **14**, 107–129.

Yoda K, Shinozaki K, Ogawa H, Hozumi K, Kira T (1965) Estimation of the total amount of respiration in woody organs of trees and forest communities. *Journal of Biology, Osaka City University*, **16**, 15–26.

Supporting Information

Additional Supporting Information may be found in the online version of this article:

Figure S1. Precipitation versus mortality by PFT.
Figure S2. Winter temperature versus mortality by PFT.
Figure S3. Summer temperature versus mortality by PFT.
Figure S4. Nitrate deposition versus mortality by PFT.
Figure S5. Sulfate deposition versus mortality by PFT.
Figure S6. Ozone versus mortality by PFT.
Figure S7. TCI versus mortality by PFT.
Figure S8. Elevation versus mortality by PFT.
Figure S9. Slope versus mortality by PFT.
Figure S10. Stand age versus mortality by PFT.
Figure S11. Radiation index versus mortality by PFT.
Figure S12. Basal area versus mortality by PFT.
Table S1. Species assignments to PFT.
Data S1. Ozone spatial model.

Please note: Wiley–Blackwell are not responsible for the content or functionality of any supporting materials supplied by the authors. Any queries (other than missing material) should be directed to the corresponding author for the article.